Progress In Electromagnetics Research B, Vol. 39, 373–392, 2012

VARIATIONAL SAR IMAGE SEGMENTATION BASED ON THE G^0 MODEL AND AN AUGMENTED LAGRANGIAN METHOD

J. L. Feng, Z. J. Cao*, and Y. M. Pi

School of Electronic Engineering, University of Electronic Science and Technology of China, Chengdu, China

Abstract—This paper present a fast algorithm for synthetic aperture radar (SAR) image segmentation based on the augmented Lagrangian method (ALM). The proposed approach considers the segmentation of SAR images as an energy minimization problem in a variational framework. The energy functional is formulated based on the statistical characteristic of SAR images. The total variation regularization is used to impose the smoothness constraint of the segmentation result. To solve the optimization problem efficiently, the energy functional is firstly modified to be convex and differentiable by using convex relaxing and variable splitting techniques, and then the constrained optimization problem is converted to an unconstrained one by using the ALM. Finally the energy is minimized with an iterative minimization algorithm. The effectiveness of the proposed algorithm is validated by experiments on both synthetic and real SAR images.

1. INTRODUCTION

Synthetic Aperture Radar (SAR) can penetrate clouds and work in nighttime, which make it becomes an important tool in remote sensing field [1]. SAR images have been applied to increasingly wide fields such as land cover classification [2], target detection [3] and information retrieval [4]. Segmentation is a key step for interpreting Synthetic Aperture Radar (SAR) images [1]. Many applications require segmenting of the SAR images for further processing. Although many approaches have been proposed to deal with it, SAR image segmentation is still a challenge task due to the complexity and low quality of SAR images.

Received 12 January 2012, Accepted 23 March 2012, Scheduled 3 April 2012

* Corresponding author: Zongjie Cao (zjcao@uestc.edu.cn).

Using of variational methods in image segmentation has been popular in past decades [5–8]. Because variational models can combine image information and prior information in a unified framework, the segmentation results are more robust compared to some classical methods. Furthermore, variational methods have solid theoretic foundation, and mature mathematical tools can be used to formulate and solve segmentation problems.

In general, to develop a variational approach for image segmentation, the energy functional is firstly defined by using various image features [9]. The minimum of the energy functional corresponds to the desired segmentation of images. Thus the problem of image segmentation is equal to an energy minimization problem. The performance of a variational segmentation approach is decided by two factors: the ability of used features to describe the image characteristics and the efficiency of the optimizing method that used to minimize the energy functional. The first one decides the effectiveness of the segmentation approach, and the second one decides the efficiency of the algorithm.

For SAR image segmentation, the statistical property of SAR image intensity or amplitude is often used to distinguish different regions. In [10, 11], Gamma distribution based variational active contour models for SAR image segmentation are presented. The authors of [12] also consider using the Weibull model. The mixture of Log-Normal model is used to separate land and water in SAR images [13]. In this paper, instead of using those models, we use the G^0 model to fit SAR data [14–16]. The reason is that among various statistical models, the G^0 model shows to be a very flexible one which can describe all kinds of surfaces. It is particularly suitable when SAR images become very heterogeneous, for example, when urban area presents in the image or the resolution is high.

Besides the definition of energy functional, another problem is how to minimize it. The efficiency of SAR image processing algorithms becomes an important issue as the rapidly increase of the amount of SAR data. Especially, application of new sensors with high-resolution cause that even one image has huge amount of data. Fast SAR image processing approaches are urgently required. For variational image segmentation, the level set method [18] is prevalent since it emerged in 1980's. However, the speed of the standard level set method is slow, which is a main obstacle for real applications [19]. Recently, there is a trend to develop efficient optimizing methods for variational image processing approaches [20–23]. Among various methods, the class of finding global minimum of variational models has drawn much attention [22, 23]. As the original energy functionals

are generally non-convex and non-differentiable, they are hard to be minimized directly. In [22, 23], the original energy functional is firstly converted to be convex and differentiable. After the converting, matured convex optimizing tools can be used to minimize the converted energy functional efficiently.

In this paper, we present a fast variational SAR image segmentation approach based on the G^0 model and the ALM. Based on the G^0 model, a variational SAR image segmentation model which uses a total variation regularized maximum likelihood formulation is proposed. Thanks to the flexibility of the G^0 model, the proposed approach can deal with SAR images with different degrees of homogenous. Then a variable splitting technique is combined with the ALM to minimize the energy functional. The efficiency of the ALM for inverse problems in image processing has been demonstrated [24, 25]. In this paper, we use the ALM to minimize the defined segmentation energy functional.

The rest of the paper is organized as follows. The SAR image segmentation problem is formulated in Section 2, in which the G^0 model is briefly introduced and the energy functional is defined. In Section 3, the ALM for constrained optimizing problems is reviewed. In Section 4 we present the proposed SAR image segmentation approach with detailed algorithm description. Section 5 provides results and discussion on both synthetic and real SAR images. Finally, this paper is concluded in Section 6.

2. VARIATIONAL SAR IMAGE SEGMENTATION MODEL

2.1. The G^0 Model of SAR Images

Due to the coherent imaging mechanism, SAR images are inevitably corrupted by speckle noise. The existence of the inherent speckle noise degrades the quality of SAR images. It blurs the edges and decreases the contrast between different regions. Moreover, the multiplicative and non-Gaussian nature precludes the adopting the state-of-the-art algorithms that designed to deal with optical images, in which the noise is often assumed to be additive Gaussian. To develop robust and effective algorithms for SAR image segmentation, the statistical property of SAR images must be taken into account.

Statistical modeling of SAR images has been an important research field for more than thirty years [1]. Goodman derived several models for SAR images: the Rayleigh distribution for single-look amplitude images, the Nakagami distribution for multi-look amplitude images and the Gamma distribution for multi-look intensity images.

Although those models are prevalent in early years, they are limited to low and middle resolution SAR images of homogenous surface. Many other models have been proposed for SAR images, such as the Log-normal distribution, the Weibull distribution and the K distribution. However, none of them are flexible enough to model all kinds of surfaces. In this paper, we use the G^0 model to describe the statistical property of SAR images. The probability distribution function of the G^0 model for amplitude and intensity SAR images can be written as [14]:

$$\begin{aligned} \text{Applitude}: p^{G^0}(z) &= \frac{2L^L\Gamma(L-\alpha)z^{2L-1}}{\gamma^\alpha\Gamma(L)\Gamma(-\alpha)(\gamma+Lz^2)^{L-\alpha}} \quad -\alpha,\gamma,L,z>0 \\ \text{Intensity}: \quad p^{G^0}(z) &= \frac{L^L\Gamma(L-\alpha)z^{L-1}}{\gamma^\alpha\Gamma(L)\Gamma(-\alpha)(\gamma+Lz)^{L-\alpha}} \quad -\alpha,\gamma,L,z>0 \end{aligned} \tag{1}$$

where L is the number of the looks, γ is the scale parameter, and α is the parameter related to the homogeneity of the observing scene: more heterogeneous scene has bigger value of α. The G^0 model has been proven to be a flexible model which can model areas with different degrees of homogeneity. Especially, it has the ability to model extremely heterogeneous areas, for which other distributions have bad fitting performance.

In real applications, the parameters of the G^0 model must be estimated from the data. Although the moment based parameter estimation method in [14] can be used, but the range of the parameter is constrained, i.e., only in case of $\alpha < -2$ correct estimation can be obtained. That will eliminate the advantage of G^0 model to describe images of extremely heterogeneous areas. Instead of using moments, the log-moment based estimator has excellent performance in multiplicative situations [16]. We adopt this method to estimate the parameters of the G^0 model. The parameters of G^0 model can be estimated by solving the following nonlinear equations:

$$\begin{cases} \ln(\gamma/L)+\psi(L)-\psi(\alpha)=c_1 \\ \psi_1(L)+\psi_1(-\alpha)=c_2-c_1 \\ \psi_2(L)-\psi_2(-\alpha)=c_3-3c_1c_2+2c_1^3 \end{cases} \tag{2}$$

where $\psi(s) = d\ln\Gamma(s)/ds$ is the digamma function and $\psi_m(s) = d^{m+1}\ln\Gamma(s)/ds^{m+1}$ is the m-th order polygamma function. The m-th order log-moment can be calculated with the data $z_1, z_2, \ldots, z_N$:

$$c_m = \frac{1}{N}\sum_{k=1}^{N}(\log z_k)^m \tag{3}$$

2.2. The Variational Formulation of SAR Image Segmentation

Based on the statistical model of SAR images, we formulate the segmentation problem in a variational framework. Let $I(\mathbf{x}) : \Omega \to R$ be the intensity SAR image, where $\Omega \subset R^2$ is the image domain. We aim to partition the SAR image into foreground area Ω_f and background area Ω_b. In both regions the gray value are assumed to follow the G^0 distribution with different parameters. Then the distribution of the image depends on the partition $\mathbf{P} = \{\Omega_f, \Omega_b\}$, which can be represented as:

$$p(I|\mathbf{P}) = \prod\nolimits_{x\in\Omega_f} p_f^{G^0}(I(\mathbf{x})|\boldsymbol{\theta}_f) \prod\nolimits_{x\in\Omega_b} p_b^{G^0}(I(\mathbf{x})|\boldsymbol{\theta}_b) \tag{4}$$

where $\boldsymbol{\theta}_k = [L_k, \gamma_k, \alpha_k]$, $k \in \{f, b\}$ represents the parameter vector of G^0 model for foreground or background area. Then segmentation of the SAR image is equal to minimize the negative likelihood of the probability $p(I|\mathbf{P})$, which is:

$$L(I|\mathbf{P}) = -\int_{x\in\Omega_f} \log\left(p_f^{G^0}(I(\mathbf{x})|\boldsymbol{\theta}_f)\right)d\mathbf{x} - \int_{x\in\Omega_b} \log\left(p_b^{G^0}(I(\mathbf{x})|\boldsymbol{\theta}_b)\right)d\mathbf{x} \tag{5}$$

The aim of segmentation is to find an optimal partition $\mathbf{P} = \{\Omega_f, \Omega_b\}$ that minimizes the likelihood. To represent the partition as variables of the likelihood explicitly, we use a region indicator function $u \in \{0, 1\}$ to represent the regions. It is defined as:

$$u(\mathbf{x}) = \begin{cases} 1 & \text{if } x \in \Omega_f \\ 0 & \text{if } x \in \Omega_b \end{cases} \tag{6}$$

Now the likelihood can be written as:

$$\begin{aligned} L(I|u) \;=\; & -\int_\Omega u(\mathbf{x}) \log\left(p_f^{G^0}(I(\mathbf{x})|\boldsymbol{\theta}_f)\right)dx \\ & -\int_\Omega (1-u(x)) \log\left(p_b^{G^0}(I(\mathbf{x})|\boldsymbol{\theta}_b\right))d\mathbf{x} \end{aligned} \tag{7}$$

We use the total variation (TV) based regularizer to impose the smoothness constraint on the segmentation result. The TV based regularization is prevalent in image restoration/reconstruction [26–28]. It is also used to regularize image segmentation problems too. The total variation norm of the function $u(\mathbf{x})$ can be written as [27]:

$$TV(u) = \int_{\Omega_f} |\nabla u(\mathbf{x})| d\mathbf{x} \tag{8}$$

Denote the negative logarithm of the probability density function as:

$$\begin{aligned}\varphi_k(\mathbf{x},\boldsymbol{\theta}_k) &= -\log\left(p_k^{G^0}(I(\mathbf{x})|\boldsymbol{\theta}_k)\right)\\ &= -\log\left(\frac{L_k^{L_k}\Gamma(L_k-\alpha_k)I(\mathbf{x})^{L_k-1}}{\gamma_k^{\alpha_k}\Gamma(L_k)\Gamma(-\alpha_k)(\gamma_k+L_kI(\mathbf{x}))^{L_k-\alpha_k}}\right), k\in[f,b] \quad (9)\end{aligned}$$

Finally, we can get the variational energy function for SAR image segmentation as:

$$\begin{aligned}E(u,\boldsymbol{\theta}_f,\boldsymbol{\theta}_b) &= \int_\Omega u(\mathbf{x})\varphi_f(\mathbf{x},\boldsymbol{\theta}_f)d\mathbf{x}+\int_\Omega(1-u(\mathbf{x}))\varphi_b(\mathbf{x},\boldsymbol{\theta}_b)d\mathbf{x}\\ &\quad +\mu\int_\Omega|\nabla u(\mathbf{x})|d\mathbf{x} \quad (10)\end{aligned}$$

The segmentation result is obtained by solving

$$\left(u^*,\,\boldsymbol{\theta}_f^*,\,\boldsymbol{\theta}_b^*\right)=\underset{\boldsymbol{\theta}_f,\,\boldsymbol{\theta}_b,\,u\in\{0,1\}}{\arg\min}\;E(u,\boldsymbol{\theta}_f,\boldsymbol{\theta}_b) \quad (11)$$

The energy functional (10) needs to be minimized with respect to region indicator function $u(\mathbf{x})$ and distribution parameters $\boldsymbol{\theta}_f$, $\boldsymbol{\theta}_b$, which is very hard to solve. A natural alternative is to minimize the energy functional iteratively. Firstly, the parameters $\boldsymbol{\theta}_f$, $\boldsymbol{\theta}_b$ are estimated with $u(\mathbf{x})$ fixed; then the indicator function $u(\mathbf{x})$ is updated with the estimated distribution parameters. Those two steps are implemented iteratively until some convergent criterion is satisfied. This kind minimization strategy is a common choice in variational image segmentation algorithms [7, 10].

The solution of the first step, i.e., minimizing (10) with respect to distribution parameters, is the maximum likelihood (ML) estimation of the parameters. However, as the ML estimation of the G^0 distribution is hard to get, so we adopt the log-moment based method to estimate the parameters in each region. This can be done by using Equation (2). The log-moment for the foreground and background can be computed by using (3), which leads to the following equations:

$$c_{f,m}=\frac{\int_\Omega\log(I(\mathbf{x}))u(\mathbf{x})d\mathbf{x}}{\int_\Omega u(\mathbf{x})d\mathbf{x}},\quad c_{b,m}=\frac{\int_\Omega\log(I(\mathbf{x}))[1-u(\mathbf{x})]d\mathbf{x}}{\int_\Omega[1-u(\mathbf{x})]d\mathbf{x}} \quad (12)$$

Then with the current estimated parameters, $u(\mathbf{x})$ is updated by minimize the energy functional with respect to $u(\mathbf{x})$. With the model parameters fixed, the gradient descent algorithm can be used to solve the minimization problem. Nevertheless, directly using of the gradient descent algorithm can be inefficient due to the non-convex and non-differentiable property of the energy functional. In this paper, those

two problems are tackled by convex relaxing and variable splitting techniques [23, 24]. As a result, the optimizing problem becomes a constrained one. Then the ALM is used to solve the constrained minimization problem efficiently. In next section, the ALM is briefly reviewed before the segmentation approach is presented.

3. THE AUGMENTED LAGRANGIAN METHOD (ALM)

The augmented Lagrangian method [29, 30] is a refinement of the penalty method (PM) [31], which is often used for solving constrained optimizing problems. They share the similarity of converting a constrained optimizing problem into an unconstrained one. But the ALM is different from the PM as it adds an additional term to the unconstrained objective function. Consider a constrained optimizing problem

$$\min f(\mathbf{v}) \quad s.t. \;\; g_k(\mathbf{v}) = 0, \quad k = 1, 2, \ldots, K \tag{13}$$

where $f(\mathbf{v})$ is the objective function, and $g_k(\mathbf{v}) = 0$ are K linear equality constraints. The penalty methods convert this constrained problem into an unconstrained one by [31]:

$$\min \Phi_n(\mathbf{v}) = f(\mathbf{v}) \; + \lambda_n \sum_{k=1}^{K} g_k(\mathbf{v})^2 \tag{14}$$

The unconstrained formulation (14) is an approximation of the original problem (13). In order to enforce the constraints exactly, the penalty function weights $\lambda_n, n = 1, 2, \ldots, N$ must be an increase sequence that goes to infinity. In real applications, finally the weights become extremely large. Unfortunately, in most cases the problem becomes more ill-conditioned as the penalty weights increase. Also, the steps for increasing λ_n must be small, making the PM less efficient.

To overcome the disadvantages of the PM, the ALM adds another term. The ALM uses the following objective function [30]:

$$\min \Phi_n(\mathbf{v}, \boldsymbol{\eta}, \lambda) = f(\mathbf{v}) + \frac{\lambda}{2} \sum_{k=1}^{K} g_k(\mathbf{v})^2 - \sum_{k=1}^{K} \eta_k g_k(\mathbf{v}) \tag{15}$$

The parameter vector $\boldsymbol{\eta} = (\eta_1, \eta_2, \ldots, \eta_K)^T$ is an estimation of the Lagrange multiplier. With the formulation (15), the optimization can be executed in an iterative way: firstly minimizing $\Phi_n(\mathbf{v}, \boldsymbol{\eta}, \lambda)$ with respect to $\boldsymbol{x}$, keeping $\boldsymbol{\eta}$ fixed; and then updating $\boldsymbol{\eta}$ according to the following equation:

$$\boldsymbol{\eta} \leftarrow \boldsymbol{\eta} - \lambda \mathbf{g} \tag{16}$$

where $\mathbf{g} = (g_1(\mathbf{v}), g_2(\mathbf{v}), \ldots, g_K(\mathbf{v}))^T$. The iteration procedure stops until some convergence criterion is satisfied. The algorithm of ALM can be summed as:

Algorithm for ALM:

1. Set $t = 0$, $\lambda > 0$ and $\boldsymbol{\eta}_0$
2. $\mathbf{v}^{t+1} = \arg\min_x \Phi(\mathbf{v}, \boldsymbol{\eta}^t, \lambda)$
3. $\boldsymbol{\eta}^{t+1} = \boldsymbol{\eta}^t - \lambda\mathbf{g}$
4. If convergence criterion is not satisfied, repeat 2 and 3.

As the ALM shows its efficiency on solving constrained optimizing problems, it has been introduced into the image processing field to solve many inverse problems [24, 25], such as the total variation based image restoration/ reconstruction and compressing sensing. Those problems are often formulated as energy minimization problems in the variational framework. The connection of the ALM and other recently proposed efficient optimizing methods has also be noticed [24]. In this paper, we use the ALM to solve the minimization problem of SAR image segmentation.

4. SAR IMAGE SEGMENTATION BASED ON THE ALM

4.1. Convex Relaxing and Variable Splitting for the Energy Model

The energy functional is minimized by iteratively estimating the distribution parameters and updating the function $u(\mathbf{x})$. By using Equations (2) and (12), the distribution parameters can be estimated accurately. This section deals with the problem of updating $u(\mathbf{x})$ with distribution parameters fixed. When the distribution parameters are fixed, the energy functional becomes:

$$E(u) = \int_\Omega u(\mathbf{x})[\varphi_f(\mathbf{x}, \boldsymbol{\theta}_f) - \varphi_b(\mathbf{x}, \boldsymbol{\theta}_b)]d\mathbf{x} + \mu \int_\Omega |\nabla u(\mathbf{x})|d\mathbf{x} + C \quad (17)$$

where $C = \int_\Omega \varphi_b(\mathbf{x}, \boldsymbol{\theta}_b)d\mathbf{x}$ is a constant. To minimize the energy functional with respect to $u(\mathbf{x})$ is equal to find a solution of the following optimization problem:

$$u^* = \arg\min_{u\in\{0,1\}} E(u) \quad (18)$$

Even when the distribution parameters are fixed, to minimize the energy functional (17) is still difficult as it is not a convex optimizing problem. The reason is that the function $u(\mathbf{x})$ takes value from the set $\{0, 1\}$ which is not convex. As a result, the minimization process can

stuck in any local minimum which correspond to bad segmentation results. Furthermore, the non-convexity of the minimizing problem also makes the adoption of efficient convex optimizing algorithms impossible. To overcome this problem, Chan et al. [22] and Bresson et al. [23] proposed a convex relaxing technique to convert the non-convex minimization problems in the form of (17) into convex ones. The admissible set of the solution is relaxed to $[0, 1]$, which is a convex set. As a result, the minimization problem becomes a convex optimization problem, which can be written as:

$$u_r^* = \arg\min_{u\in[0,1]} E(u) \tag{19}$$

where the energy function is in the form of Equation (17). The solution of the relaxed minimization problem and the solution of the original problem are related by the following theorem [22, 23]:

Theorem 1: If u_r^* is any minimizer of (19), it is a global minimizer of (19) because of the convexity of the minimization problem. Moreover, for almost every $\xi \in (0, 1)$, the threshold function

$$u^*(\mathbf{x}) = \begin{cases} 1, & \text{if } u_r^*(\mathbf{x}) > \xi \\ 0, & \text{otherwise} \end{cases} \tag{20}$$

is also global minimizer of (19), and the original problem (18) as well.

According to Theorem 1, we can solve the relaxed minimization problem (19) instead of solving the original problem (18). Because of the convexity, the result is not affected by the minimization strategy. A simple algorithm is the gradient descent method which is widely used. Nevertheless, because of the L_1 norm of the gradient of $u(\mathbf{x})$ in the total variation term, the energy functional is non-differentiable and gradient descent algorithm will very slow due to the need of regularization in numerical realization. So the variable splitting technique is used to avoid this problem [24]. This is done by introducing a new vectorial function $\mathbf{d}(\mathbf{x})$ as follows:

$$\begin{aligned} E(u, \mathbf{d}) \;=\; & \int_\Omega u(\mathbf{x})\varphi_f(\mathbf{x}, \boldsymbol{\theta}_f)d\mathbf{x} + \int_\Omega (1 - u(\mathbf{x}))\varphi_b(\mathbf{x}, \boldsymbol{\theta}_b)d\mathbf{x} \\ & + \mu \int_\Omega |d(\mathbf{x})|d\mathbf{x} \qquad \text{such that} \quad \mathbf{d}(\mathbf{x}) = \nabla u(\mathbf{x}) \end{aligned} \tag{21}$$

By doing this, the energy functional is differentiable now. And the minimization of the energy functional becomes a constrained optimizing problem, which can be solved with the ALM.

4.2. Use of the ALM

The ALM in Section 3 uses scalar valued linear constraints. However, in the SAR image segmentation energy model, the equality constraint

is vector valued, and is defined on the continuous image domain. That means the number of the constraints is infinite. Thus some adaptation of the ALM is required.

For the vector $\mathbf{p}$ and $\mathbf{q}$, denote $(\mathbf{p}, \mathbf{q})$ and $||\mathbf{p}||_2$ the Euclidean inner product and the L_2 norm respectively. Let $\mathbf{v} = [u \ \mathbf{d}]$, $\mathbf{g}(\mathbf{v}) = \mathbf{d} - \nabla u$, then the constraint $\mathbf{d}(\mathbf{x}) = \nabla u(\mathbf{x})$ is the same as $\mathbf{g}(\mathbf{v}(\mathbf{x})) = 0$. The unconstrained object function of the ALM method for Equation (21) is:

$$\Phi(\mathbf{v}, \boldsymbol{\eta}) = E(\mathbf{v}) + \frac{\lambda}{2}\int_\Omega ||\mathbf{g}(\mathbf{v}(\mathbf{x}))||_2^2 d\mathbf{x} - \int_\Omega (\boldsymbol{\eta}(\mathbf{x}), \mathbf{g}(\mathbf{v}(\mathbf{x})))\, d\mathbf{x} \quad (22)$$

The first term in the right side is the SAR image segmentation energy functional. The second and the third term are the penalty term and the augmented Lagrangian term respectively. Compared to Equation (15), the integration is used instead of the summation as the constraint is defined on the continuous image domain. And the L_2 norm and inner product is used to impose the constraint $\mathbf{g}(\mathbf{v}(\mathbf{x})) = 0$ as the constraint at each pixel is vector valued.

To minimize the unconstraint object function (22), let us rewrite it as:

$$\begin{aligned}\Phi(u, \mathbf{d}, \boldsymbol{\eta}) \ = \ & E(u, \mathbf{d}) + \frac{\lambda}{2}\int_\Omega ||\mathbf{d}(\mathbf{x}) - \nabla u(\mathbf{x})||_2^2 d\mathbf{x} \\ & - \int_\Omega \boldsymbol{\eta}(\mathbf{x})^T(\mathbf{d}(\mathbf{x}) - \nabla u(\mathbf{x}))dx \end{aligned} \quad (23)$$

The goal is to find the optimal solution $(u^*, \mathbf{d}^*, \boldsymbol{\eta}^*)$ which minimize $\Phi(u, \mathbf{d}, \boldsymbol{\eta})$. Because the variable u and $\mathbf{d}$ is decoupled in the energy functional $E(u, \mathbf{d})$, the minimization procedure can be decomposed into the following iteratively solved subproblems by using the algorithm of ALM:

$$\begin{cases} u^{t+1} = \arg\min\limits_{u\in[0,1]} \displaystyle\int_\Omega u(\mathbf{x})\varphi_f(\mathbf{x}, \boldsymbol{\theta}_f)d\mathbf{x} + \int_\Omega (1-u(\mathbf{x}))\varphi_b(\mathbf{x}, \boldsymbol{\theta}_b)d\mathbf{x} \\ \qquad + \dfrac{\lambda}{2}\displaystyle\int_\Omega ||\mathbf{d}(\mathbf{x})^t - \nabla u(\mathbf{x})||_2^2 d\mathbf{x} - \int_\Omega \left(\boldsymbol{\eta}(\mathbf{x})^t\right)^T(\mathbf{d}(\mathbf{x}) - \nabla u(\mathbf{x}))dx \\ \mathbf{d}^{t+1} = \arg\min\limits_{d} \mu\displaystyle\int_\Omega |d(\mathbf{x})|d\mathbf{x} + \frac{\lambda}{2}\int_\Omega ||\mathbf{d}(\mathbf{x}) - \nabla u^{t+1}(\mathbf{x})||_2^2 d\mathbf{x} \\ \qquad - \displaystyle\int_\Omega \left(\boldsymbol{\eta}(\mathbf{x})^t\right)^T(\mathbf{d}(\mathbf{x}) - \nabla u^{t+1}(\mathbf{x}))dx \\ \boldsymbol{\eta}(\mathbf{x})^{t+1} = \boldsymbol{\eta}(\mathbf{x})^t - \lambda\left(\mathbf{d}(\mathbf{x})^{t+1} - \nabla u(\mathbf{x})^{t+1}\right) \end{cases} \quad (24)$$

For the first subproblem, the optimal condition is:

$$\begin{aligned}\lambda\Delta u^{t+1}(\mathbf{x}) &= \varphi_f(\mathbf{x},\boldsymbol{\theta}_f)-\varphi_b(\mathbf{x},\boldsymbol{\theta}_f)\\ &\quad +\lambda div(\mathbf{d}(\mathbf{x})^t)-div(\boldsymbol{\eta}(\mathbf{x})^t), \qquad u\in[0,1] \quad (25)\end{aligned}$$

This equation can be solved by the Gauss-Seidel iteration efficiently. Denote the right side of the equation as $r(\mathbf{x})$, then for every pixel $\mathbf{x}=(i,j)$, the function $u(\mathbf{x})$ is updated by:

$$\begin{aligned}uu(i,j) &= \frac{1}{4}\Bigg(u^{t+1,\,n}(i-1,\,j)+u^{t+1,\,n}(i,j-1)+u^{t+1,n}(i+1,j)\\ &\quad +u^{t+1,\,n}(i,j+1)-\frac{1}{\lambda}r(i,j)\Bigg)\\ u^{t+1,\,n+1} &= \max\left\{\min\left\{uu,1\right\},0\right\} \qquad (26)\end{aligned}$$

where $n=0,1,2\ldots$ is the number of iteration and $u^{t+1,\,0}=u^t$. The second equation is used to ensure that $u\in[0,1]$.

For the second subproblem, the closed form solution can be obtained as:

$$\mathbf{d}(\mathbf{x})^{t+1}=\frac{\nabla u(\mathbf{x})^{t+1}+\lambda^{-1}\boldsymbol{\eta}(\mathbf{x})^t}{||\nabla u(\mathbf{x})^{t+1}+\lambda^{-1}\boldsymbol{\eta}(\mathbf{x})^t||_2}\max\left(||\nabla u(\mathbf{x})^{t+1}+\lambda^{-1}\boldsymbol{\eta}(\mathbf{x})^t||_2-\lambda^{-1}\mu,0\right) \quad (27)$$

At last, the third subproblem is computed directly.

4.3. The Algorithm

The proposed G^0 model and ALM based SAR image segmentation approach can be summarized as:

Algorithm for SAR image segmentation based on G^0 model and ALM:

1. Initialize the region indicator function u^0, set parameters μ, λ, TOL_i, TOL_o, let $k=0$
2. Estimate the G^0 model parameters $\boldsymbol{\theta}_f^{k+1}$, $\boldsymbol{\theta}_b^{k+1}$ with (2) and (12)
3. Solve (19) by using the ALM
   1). Let $t=0$, $u^{k+1,0}=u^t$, $\mathbf{d}^0=\nabla u^t$, $\boldsymbol{\eta}^0=0$
   2). Compute $u^{k+1,\,t+1}$ with Equation (26)
   3). Compute $\mathbf{d}^{t+1}$ with Equation (27)
   4). Compute $\boldsymbol{\eta}^{t+1}$ with the third equation in Equation (25)
   5). If $\int_\Omega \left|u^{k+1,t+1}(\mathbf{x})-u^{k+1,t}(\mathbf{x})\right| d\mathbf{x} > TOL_i$, repeat 2).–5).; otherwise, $u^{k+1}=Th(u^{k+1,\,t+1})$

4. If $\int_\Omega \left|u^{k+1}(\mathbf{x}) - u^k(\mathbf{x})\right| d\mathbf{x} > TOL_o$, go to 2; otherwise, stop the algorithm.

The parameter TOL_i, TOL_o is the error tolerance that used to test the convergence condition for the inner and outer iteration. And the function $Th(\cdot)$ is the threshold function (20) with $\xi = 1/2$.

5. EXPERIMENTAL RESULTS

In this section, the performance of the proposed SAR image segmentation approach is validated by experiments on both synthetic and real SAR images. All experiments are performed on a Pentium(R) Dual-Core 2.7 GHz workstation under Windows XP professional without any particular code optimization. The parameters need to be specified for numerical realization of the algorithm. The parameter μ controls the smoothness of the segmentation results. Bigger value of μ is required for smoother segmentation results. The parameter λ has significant impact on the speed of the algorithm. Too small or too big value of λ will slow down the algorithm. The parameters TOL_i, TOL_o have little effect on the segmentation results when they are small enough. But when they are too small, the algorithm needs much more iterations to get convergent. Following those principles, the parameters are generally set as $\mu = 0.1$, $\lambda = 1$, $TOL_i = TOL_o = 0.1$ if there is no special declaration. Those parameters are found to give good segmentation results for most situations. Nevertheless, those parameters are still need adjustment to get optimal segmentation performance.

5.1. Simulated Data

In this section, simulated SAR images are used to test the proposed approach. First, to show the advantage of using the G^0 model, we compare segmentation results by using the G^0 model with results by using the Gamma model. This is done by replacing the G^0 model with the Gamma model in the proposed approach. About the expression and parameter estimation of the Gamma model, we refer to [1]. The comparison is made by using three synthetic images.

The used three images are generated according to the G^0 model. The number of looks is fixed to 4 for all images. The mean amplitude is 64 for the foreground region, 144 for the background region. The roughness parameter α is set to be $\{-25, -5, -1.5\}$ for three images respectively. When $\alpha = -25$, the simulated data is of low roughness, and the G^0 model is very like Gamma model. That means the Gamma model can fit the data well. However, with the value of

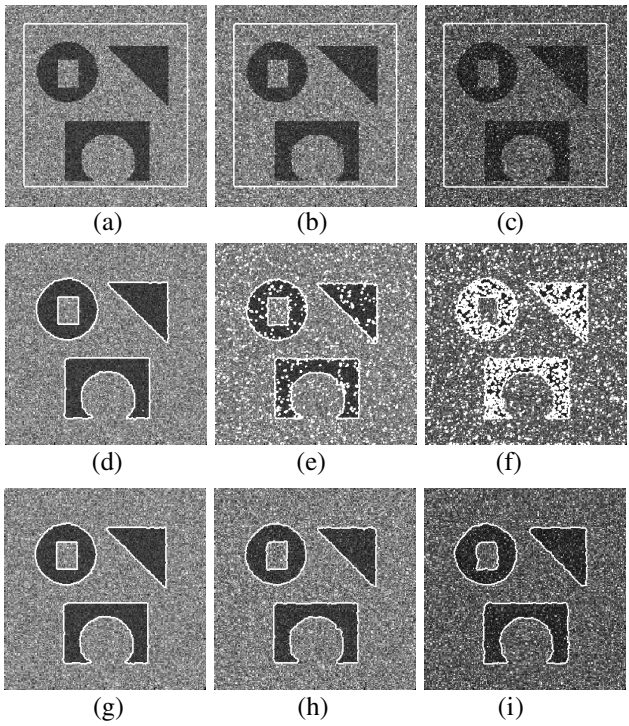

Figure 1. Segmentation results with the Gamma model and G^0 model. (a)–(c) Initial segmentation. (d)–(f) Segmentation results with Gamma model. (g)–(i) Segmentation results with G^0 model.

α increases, the Gamma model is more and more incapable to fit the data. The simulated images are shown as Figs. 1(a)–(c) with the initial segmentation represented by the white rectangle. The final segmentations for the G^0 model based approach are shown as Figs. 1(d)–(f). Figs. 1(g)–(i) are the results with the Gamma model.We can observe that the Gamma based approach can give good result when the image is of low roughness. But as the degree of the roughness increases, the Gamma model based approach is not suitable. However, with the G^0 model, satisfied segmented results are obtained for all three images.

We also give the segmentation accuracy in Table 1. The segmentation accuracy is defined as:

$$SA = \frac{Num(\Omega_f \cap \Omega_f^S) + Num(\Omega_b \cap \Omega_b^S)}{Num(\Omega)} \times 100$$

where Ω_f, Ω_b are the two regions of the ground truth image, and Ω_f^S,

Table 1. Segmentation accuracy comparison of Fig. 1.

	$\alpha = -25$	$\alpha = -5$	$\alpha = -1.5$
The Gamma Model Based Approach	99.12	97.41	94.33
The G^0 Model Based Approach	99.03	98.87	98.14

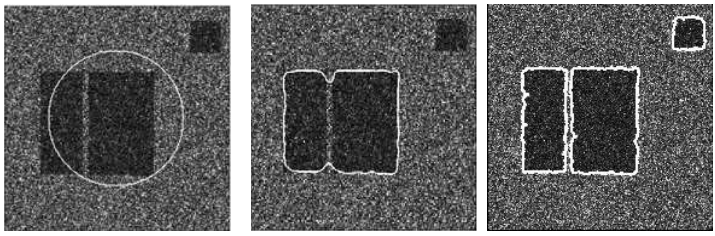

(a) (b) (c)

Figure 2. Comparison of segmentation results with level set method and ALM. (a) The initial segmentation. (b) Segmentation result with the level set method. (c) Segmentation result with the ALM.

Ω_b^S are the segmented regions. $Num(\cdot)$ is the total pixels in that region. The comparison result shows that the G^0 model based approach is more flexible than the Gamma model based approach to cope with images with different degree of roughness.

The next experiment is performed to show the advantage of using the ALM instead of the level set method. The level set method is a popular tool for variational image segmentation. In [17], the level set method is used to minimize the G^0 model energy model. To show the advantage of using the ALM for energy minimization, a simulated image is used to compare the performance of the proposed method and the method in [17]. The results are shown in Fig. 2. The segmentation result with the level set method is not satisfactory as the narrow channel between two rectangles and the small rectangle far from the initial curve is not detected. This is because that at each iteration, the energy functional is not convex with respect to the level set function, which makes the evolving contour sticking in some local minimums which correspond to the bad segmentation results. On the contrary, the proposed ALM based approach can get good segmentation result. The two regions are separated well. The reason is that adoption of the convex relaxing technique can alleviate the problem caused by local minimum.

5.2. Real Data

We also test the proposed approach on various real SAR images. Four real amplitude SAR images are chosen. The first one is a COSMO-SkyMed multilook SAR image with a lake located in the center. The second one is a single look SAR image chip picked out from the MSTAR public dataset. The other two SAR images are obtained by domestic airborne SAR sensors. Except the first one, the other three images are with resolution less than 1 m. The information about the used SAR images is given in Table 2.

Figure 3 shows the segmentation result of the four real SAR images with the proposed method. The Gamma model is also used to model those images and the segmentation results with the Gamma model are demonstrated for comparison too. As we can see, for the first two images, both of G^0 model based approach and Gamma based approach can get good segmentation results. Only slight difference can be observed. For the lake image, the multilook processing reduces the resolution, making the SAR image very homogenous. So the Gamma model has good fit performance to this SAR image. The MSTAR dataset is collected by the Sandia National laboratories for automatic target recognition (ATR). Each target chip contains three parts: target, shadow and background. Segmentation of the target chips are used for extracting target information such as the orientation and shape of targets. As the proposed method is a two region segmentation approach, only the target part is extracted in this study. There are many researches show that the Gamma model is a suitable model for modeling the MSTAR deta. Nevertheless, as the segmentation results shown, good segmentation results can also be obtained by using the G^0 model.

Two domestic high-resolution SAR images are also used test the

Table 2. Information of the used SAR images.

Image	Size	Band	Polarization Type	ENL	Image Source
Lake	257×260	X	HH	14.915	ASI
Target 1	128×128	X	HH	5.138	Sandia National Laboratories
Target 2	437×403	X	HH	2.727	A domestic airborne radar imaging data
Airplane	128×218	X	HH	2.199	A domestic airborne radar imaging data

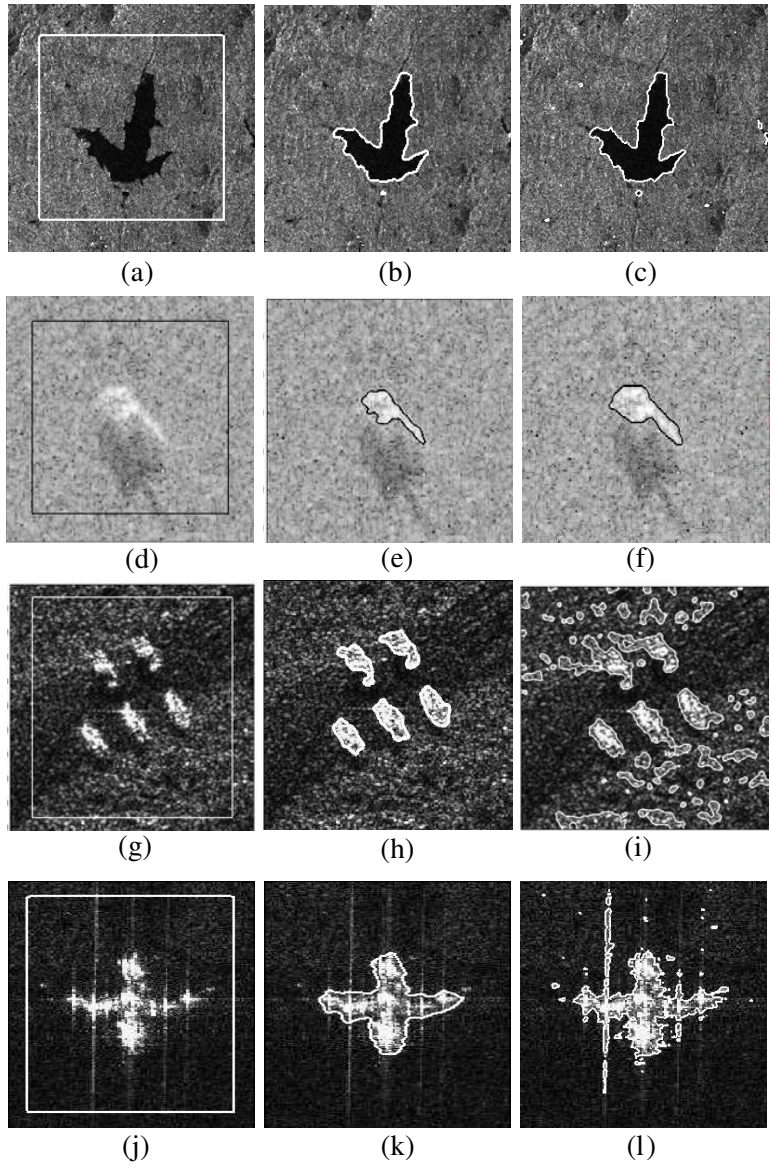

Figure 3. Segmentation results of three real SAR images with the proposed approach and the Gamma based approach. (a), (d), (g), and (j): The initialization segmentation. (b), (e), (h), and (k): Segmentation results with the proposed approach. (c), (f), (i), and (l): Segmentation results with the Gamma model and the ALM.

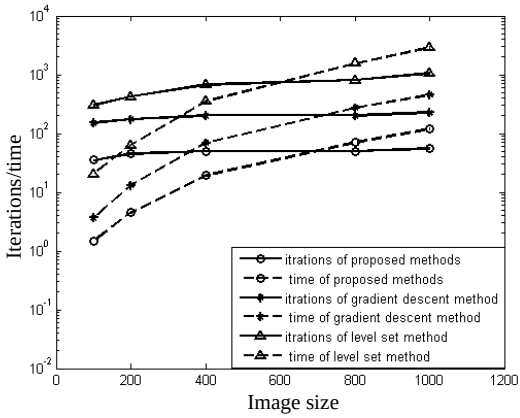

Figure 4. Computation time and iterations comparison: The solid line shows the iterations needed for each method to converge to segmentation result (in times), the dashed lines show the corresponding computation time (in seconds).

algorithm. The resolution is less than 1 m for both SAR images. It can be observed that due to the high resolution, strong reflectors and textures are presented in the SAR image, which makes the SAR images more heterogeneous. Using the G^0 distribution to model the SAR image respectively, the segmentation results are shown in Figs. 3(h) and (k). The results obtained by using the Gamma model is shown in Figs. 3(i) and (l). The results demonstrate that with the G^0 model, targets are detected without false alarm. But with Gamma model, many pixels with brighter gray level are segmented to be target pixel. It is clearly shows that by introducing the G^0 model into the energy functional, the proposed method is more suitable for segmentation high-resolution SAR images. The results demonstrate the effectiveness of the proposed approach and it's adaptively to different kinds of SAR images.

At last, to show the computational efficiency of the proposed approach compared to the level set based SAR image segmentation approaches, we resize the image of Fig. 1(b) to different scales and run different approaches on those images. The proposed ALM based approach and the level set based approach is applied. Moreover, we also minimize the energy functional (17) with the gradient descent algorithm. The number of iterations and the time consuming that needed for the algorithm convergence of each method are shown in Fig. 4. It's find that the proposed method needs less iterations and computational time compared to the other two methods. This justifies the using of the ALM for energy minimization.

6. CONCLUSION

We present a variational SAR image segmentation approach based on the G^0 statistical model and the augmented Lagrangian method. The flexibility of the G^0 model makes that the proposed approach can adaptively deal with different kinds of SAR images. The ALM is used to minimize the relaxed convex energy in the segmentation procedure. Compared to the level set based approaches, the proposed approach is less likely to fall into local minimums. The proposed approach is also proved to be faster compared to the level set method based SAR image segmentation approaches.

ACKNOWLEDGMENT

This work is supported by the National Natural Science Foundation of China under Projects 60802065 and the Fundamental Research Funds for the Central Universities under Projects ZYGX2009Z005.

REFERENCES

1. Oliver, C. and S. Quegan, *Understanding Synthetic Aperture Radar Images*, Artech House, Norwood, MA, 1998.
2. Mishra, P., D. Singh, and Y. Yamaguchi, "Land cove classification of PALSAR images by knowledge based decision tree classifier and supervised classifiers based on SAR observation," *Progress In Electromagnetics Research B*, Vol. 30, 47–70, 2011.
3. Tian, B., D.-Y. Zhu, and Z.-D. Zhu, "A novel moving target detection approach for dual-channel SAR system," *Progress In Electromagnetics Research*, Vol. 115, 191–206, 2011.
4. Jin, Y.-Q., "Polarimetric scattering modeling and information retrieval of SAR remote sensing — A review of FDU work," *Progress In Electromagnetics Research*, Vol. 104, 333–384, 2010.
5. Caselles, V., R. Kimmel, and G. Sapiro, "Geodesic active contours," *Int. J. Computer Vision*, Vol. 22, No. 1, 61–79, 1997.
6. Zhu, S. C. and A. Yuille, "Region competition: Unifying snakes, region growing, and Bayes/MDL for multiband image segmentation," *IEEE Trans. Pattern Anal. Mach. Intell.*, Vol. 18, No. 9, 884–900, Sept. 1996.
7. Chan, T. and L. Vese, "Active contour without edges," *IEEE Trans. Image Process.*, Vol. 10, No. 2, 266–277, 2001.

8. Paragios, N. and R. Deriche, "Geodesic active regions and level set methods for supervised texture segmentation," *Int. J. Computer Vision*, Vol. 46, No. 3, 223–247, 2002.
9. Cremers, D., M. Rousson, and R. Deriche, "A review of statistical approaches to level set segmentation: integrating color, texture, motion and shape," *Int. J. Computer Vision*, Vol. 72, No. 2, 195–215, 2007.
10. Ayed, I. B., A. Mitiche, and Z. Belhadj, "Multiregion level-set partitioning of synthetic aperture radar images," *IEEE Trans. Pattern Anal. Mach. Intell.*, Vol. 27, No. 5, 793–800, 2005.
11. Shuai, Y., H. Sun, and G. Xu, "SAR image segmentation based on level set with stationary global minimum," *IEEE Geosci. Remote Sens. Lett.*, Vol. 5, No. 4, 644–648, 2008.
12. Ayed, I. B., N. Hennane, and A. Mitiche, "Unsupervised variational image segmentation classification using a Weibull observation model," *IEEE Trans. Image Process.*, Vol. 15, No. 11, 3431–3439, 2006.
13. Silveira, M. and S. Heleno, "Separation between water and land in SAR image using region based level set," *IEEE Trans. Geoscience and Remote Sensing*, Vol. 6, No. 3, 471–475, 2009.
14. Frery, A. C., H. J. Muller, C. C. F. Yanasse, and S. J. S. Sant'Anna, "A model for extremely heterogeneous clutter," *IEEE Trans. Geoscience and Remote Sensing*, Vol. 35, No. 3, 648–659, 1997.
15. Frery, A. C. and F. Yanasse, "Alternative distributions for the multiplicative model in SAR images," *International Geoscience and Remote Sensing Symposium*, Vol. 1, 169–171, 1995.
16. Tison, C., J.-M. Nicolas, F. Tupin, and H. Maitre, "A new statistical model for Markovian classification of urban areas in high-resolution SAR images," *IEEE Trans. Geoscience and Remote Sensing*, 2046–2057, Vol. 42, No. 10, 2004.
17. Feng, J., Z. Cao, and Y. P, "A G^0 statistical model based level set approach for SAR image segmentation," *Proc. EUSAR*, 841–844, 2010.
18. Malladi, R., J. A. Sethian, and B. C. Vemuri, "Shape modeling with front propagation: A level set approach," *IEEE Trans. Pattern Anal. Mach. Intell.*, Vol. 17, No. 2, 158–175, 1995.
19. Li, C., C. Xu, C. Gui, and M. D. Fox, "Level set evolution without re-initialization: A new variational formulation," *Proc. CVPR*, Vol. 1, 430–436, 2005.

20. Goldenberg, R., R. Kimmel, E. Rivlin, and M. Rudzsky, "Fast geodesic active contours," *IEEE Trans. Image Process.*, Vol. 10, No. 10, 1467–1475, 2001.
21. Shi, Y. and W. C. Karl, "A real-time algorithm for the approximation of level-set-based curve evolution," *IEEE Trans. Image Process.*, Vol. 17, No. 5, 645–656, 2008.
22. Chan, T. F., S. Esedoglu, and M. Nikolova, "Algorithms for finding global minimizers of image segmentation and denoising models," *SIAM J. Appl. Math*, Vol. 66, No. 5, 1632–1648, 2006.
23. Bresson, X., S. Esedoglu, P. Vandergheynst, et al., "Fast global minimization of the active contour/snake model," *J. Math. Imaging. Vision.*, Vol. 28, No. 2, 151–167, 2007.
24. Wu, C. and X. C. Tai, "Augmented lagrangian method, dual methods, and split Bregman iteration for ROF, vectorial TV, and high order models," *SIAM J. Imaging Sci.*, Vol. 3, No. 3, 300–339, 2010.
25. Afonso, M. V., J. M. Bioucas-Dias, and M. A. T. Figueiredo, "An augmented lagrangian approach to the constrained optimization formulation of imaging inverse problems," *IEEE Trans. Image Process.*, Vol. 20, No. 3, 681–695, 2011.
26. Chambolle, A., "An algorithm for total variation minimization and application," *J. Math. Imaging. Vision.*, Vol. 20, Nos. 1–2, 89–97, 2004.
27. Rudin, L., S. Osher, and E. Fatemi, "Nonlinear total variation based noise removal algorithms," *Physica D*, Vol. 60, 259–268, 1992.
28. Beck, A. and M. Teboulle, "Fast gradient-based algorithms for constrained total variation image denosing and deblurring problems," *IEEE Trans. Image Process.*, Vol. 18, No. 11, 2419–2434, 2009.
29. Nocedal, J. and S. J. Wright, *Numerical Optimization*, 2nd Edition, Springer-Verlag, New York, 2006.
30. Powell, M., "A method for nonlinear constraints in minimization problems," *Optimization*, R. Fletcher Edition, 283–298, Academic, New York, 1969.
31. Bertsekas, D. P., "Multiplier methods: A survey," *Automatica*, Vol. 12, 133–145, 1976.